EUMETSAT ECMWF

EUMETSAT/ECMWF Fellowship Programme Research Report

58

Towards assimilating surface sensitive microwave channels over land

Katrin Lonitz, Alan J. Geer and Niels Bormann

March 2022

Series: EUMETSAT/ECMWF Fellowship Programme Research Reports

A full list of ECMWF Publications can be found on our web site under:
http://www.ecmwf.int/en/publications/

Contact: library@ecmwf.int

European Centre for Medium Range Weather Forecasts, Shinfield Park, Reading, RG2 9AX, UK

Abstract

Microwave channels with a low sensitivity to the surface are assimilated over ocean and land. However, challenges in the description of the land properties (e.g. surface emissivity) mean that surface sensitive microwave channels have, until now, only been assimilated over ocean. In this study we investigate the possibility of assimilating surface sensitive microwave channels over land using the all-sky approach. An emissivity retrieval has typically been used to provide the surface emissivity when assimilating the less surface sensitive microwave frequencies. It is difficult to apply this to the surface sensitive microwave channels in our system, as the bias correction over ocean is affected by assimilation over land, and this interaction results in a moistening of the surface humidity over tropical ocean. We propose to use a spectrally adjusted emissivity retrieval: an emissivity retrieval at 19 v GHz which is adjusted using the dependency of emissivity with frequency obtained from an atlas. In our setup we assimilate additionally 89/92 GHz and 150/166 GHz from GMI and SSMIS-F17, and 183 GHz channels from GMI over land. The results are quite neutral with small positive improvements in the observational fits to AMSU-A and surface AMVs. However, there remains a need to improve the bias predictors when assimilating microwave radiances over land, to resolve issues over arid land surfaces and to allow the assimilation of 89/92 GHz channels from MWRI and AMSR2.

1 Background

The all-sky assimilation of surface sensitive microwave channels over ocean has been done operationally at ECMWF since 2009 [Bauer et al., 2010, Geer and Bauer, 2011]. However, assimilation over land has proven more challenging due to uncertainties in the emissivity and skin temperature, especially for surface sensitive channels. All-sky assimilation adds the difficulty of separating errors in cloud and precipitation from those in the description of the surface. Unfortunately, there is no physically based emissivity model in place for the assimilation of microwave frequencies over land. Over ocean, the physically-based emissivity model in FASTEM [English and Hewison, 1998] has been very successful, but over land, the semi-empirical FASTEM-land emissivity model still has too many uncertainties to be used successfully. To overcome this hurdle, a land surface emissivity retrieval [Karbou et al., 2006] has been utilised for less surface sensitive channels. Traditionally, this was done using a clear-sky radiative transfer model, along with cloud screening. To apply this approach to all-sky conditions, Baordo and Geer [2016] have used all-sky radiative transfer to enable a dynamic emissivity retrieval in conditions of semi-transparent clouds and, hence, to allow all-sky assimilation over land for 183 GHz channels such as those on SSMIS-F17, and 119 GHz channels from MWHS-2 [Lawrence et al., 2018]. In very convective situations with heavy precipitation the surface becomes invisible and values from an emissivity atlas are taken instead.

An accurate estimate of surface emissivity is instrumental when trying to assimilate microwave frequencies over land, especially when attempting the assimilation of surface-sensitive channels. This is because the brightness temperatures observed over land are often more strongly influenced by the surface rather than by hydrometeors in the atmosphere. This means that, when attempting to extract atmospheric signals from the brightness temperature, the accurate description of surface properties is even more crucial over land than it is over ocean. Additionally, skin temperature over land is less well known than over ocean. These large uncertainties in skin temperature and emissivity make it challenging to assimilate surface-sensitive observations over land (e.g., English [2008]).

In this work, we focus on the development of an accurate land surface emissivity estimate which can be used for the assimilation of surface sensitive microwave channels. We introduce a new idea to obtain emissivity over land, a spectrally adjusted emissivity retrieval which can be used for all microwave fre-

quencies under clear and cloudy conditions. We also test which microwave frequencies contain enough atmospheric signal (water vapour, clouds, precipitation) over land. In future, it is desirable to assimilate those surface sensitive microwave channels not just for their atmospheric information but also for the land information (e.g. soil moisture), which would be an improvement over using external satellite products.

In a more recent study by Geer et al. [2022] the assimilation of surface sensitive microwave radiances was tested for implementation in IFS model cycle 48R1. Geer et al. [2022] use the spectrally adjusted emissivity retrieval developed in this work to assimilate microwave radiances over land, with an enhancement to more frequencies and more instruments, besides adding new bias predictors. With these innovations the operational assimilation of mid-frequency microwave window channels over land has become possible for the first time.

2 Offline Experiment

To get a better idea of the sensitivity of microwave brightness temperatures to differences in surface properties and atmospheric conditions, with and without hydrometeors, we have set up an offline experiment. This offline experiment runs the RTTOV SCATT forward model from the RTTOV package 12.1 [Saunders et al., 2018] to simulate the effects of ocean, forest, grass and soil surfaces with varying amounts of hydrometeors in the atmosphere. The emissivity of the ocean and land surfaces have been set using the FASTEM input model parameters [English and Hewison, 1998]. Four hydrometeor types (liquid cloud, rain, ice cloud and snow) are subsequently added to a clear-sky standard RTTOV test profile while keeping temperature and humidity (unrealistically) constant. With this setup we are able to isolate the effect of hydrometeors on the brightness temperatures over varying surface conditions.

The atmospheric profiles for the different scenarios are shown in Fig.1. The cloud cover (bottom left panel) is representative for the end scenario after adding liquid cloud water, rain, cloud ice and snow. The liquid cloud profile can be found in black in the top right panel, which is later complemented by rain (black line in the bottom right panel). Finally, ice (red dashed line in top right panel) and snow (red dashed line in bottom right panel) are added. Fig. 2 shows the brightness temperatures for GMI-like channels in clear sky conditions for the different surfaces. As expected the emissivities are much lower for the ocean than for the land surfaces, which gives a profound effect on the brightness temperatures. Also the emissivities over land show a much smaller dependency on frequency than is seen over ocean. There is also a polarisation difference in the surface emissivity over land that could in future be exploited at low frequencies to detect the unpolarised signal from cloud and precipitation.

Fig. 3 lets us study the frequency dependence of the effect of hydrometeors over ocean and land surfaces. Here, examples over ocean (Fig. 3a, Fig. 3b) and forest (Fig. 3c, Fig. 3d) are chosen. The biggest differences in the change in brightness temperatures can be seen when comparing the different surfaces, i.e. comparing Fig. 3a with Fig. 3c or Fig. 3b with Fig. 3d. A smaller difference can be found between the profiles with different hydrometeors, i.e. comparing Fig. 3a with Fig. 3b or Fig. 3c with Fig. 3d. The addition of hydrometeors shows large differences in brightness temperatures of up to 40 K over ocean, whereas over forest brightness temperatures only change by 8 K. For the other surfaces (grass and soil) the signal is similar. Over ocean, the differences in brightness temperature are largest (reaching 45 K) at frequencies up to 89 GHz, whereas at higher frequencies the change is smaller (less than 10 K; Fig. 3a). Over forest, the effect of adding hydrometeors is different. Figure 3d shows that the difference in brightness temperature for low frequencies (37 GHz and lower) is only 1 K to 2 K. For higher frequencies the differences reach 3 K at 89 GHz, 5 K at 183 GHz, and 8 K at 166 GHz. These signals are mostly a

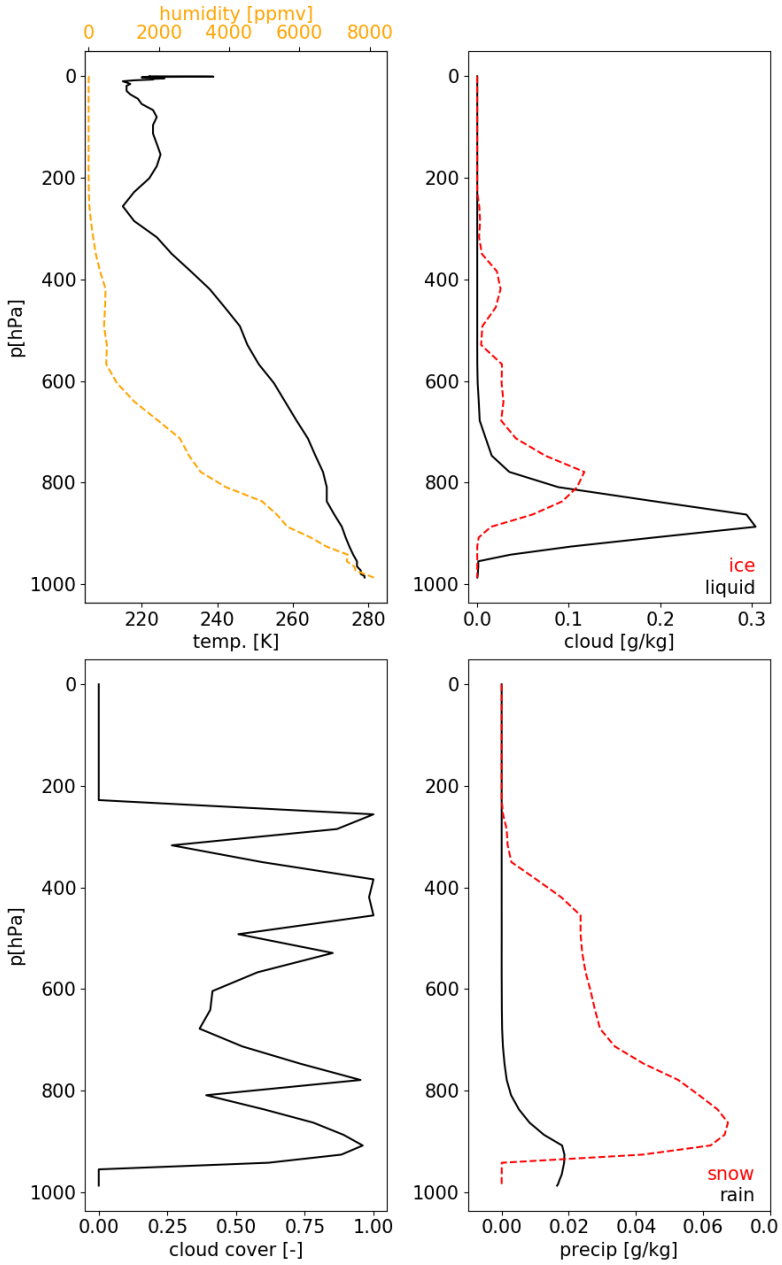

Figure 1: Top left: Vertical profiles of temperature (solid black line) and humidity (dashed yellow line). Top right: Vertical profile of cloud liquid water (solid black line) and cloud ice (dashed red line). Bottom left: Vertical profile of cloud cover. Bottom right: Vertical profile of rain (solid black line) and snow (dashed red line).

reduction in brightness temperatures due to the scattering effects of ice and snow hydrometeors.

In summary, the biggest impact of hydrometeors on brightness temperatures is over ocean at lower frequencies. The impact is less at higher frequencies but its magnitude is more similar between land and ocean. The effect of the atmosphere and of hydrometeors is smallest at low frequencies (37 GHz and

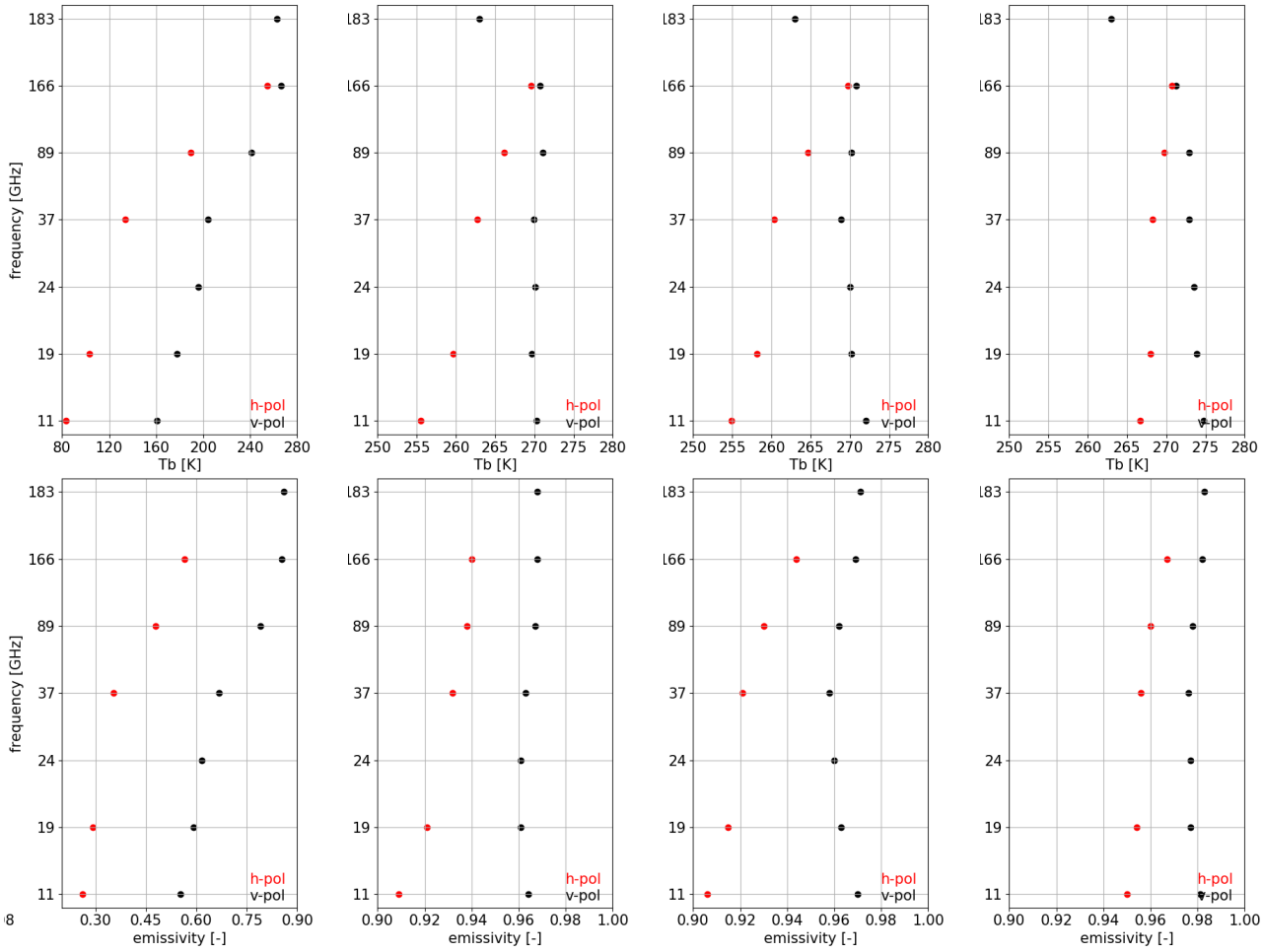

(a) Ocean (b) Soil (c) Grass (d) Forest

Figure 2: Brightness temperature (top row) and emissivity (bottom row) for each GMI-like channel for different surfaces a) ocean, b) soil, c) grass and d) forest under clear-sky conditions. Note: x-axes in a) are for longer range than in b), c) and d).

lower) over land. This means that when assimilating microwave observations to improve atmospheric initial conditions over land surfaces, the best frequencies are probably at 89 GHz and higher. Hence, for the remainder of this study we focus on the assimilation of these channels.

However, this conclusion is based on atmospheric profiles with a moderate amount of rain or snow. In heavy convective systems with larger hydrometeor amounts, the atmospheric signal can be large even at low frequencies over land. Such situations are most likely to be found in frontal systems and the intertropical convergence zone (ITCZ). Hence, after the successful testing of the land assimilation of microwave brightness temperatures at 89 GHz and higher in this work, it was worth going a step further and assessing the assimilation of lower frequencies, as done in e.g. Geer et al. [2022].

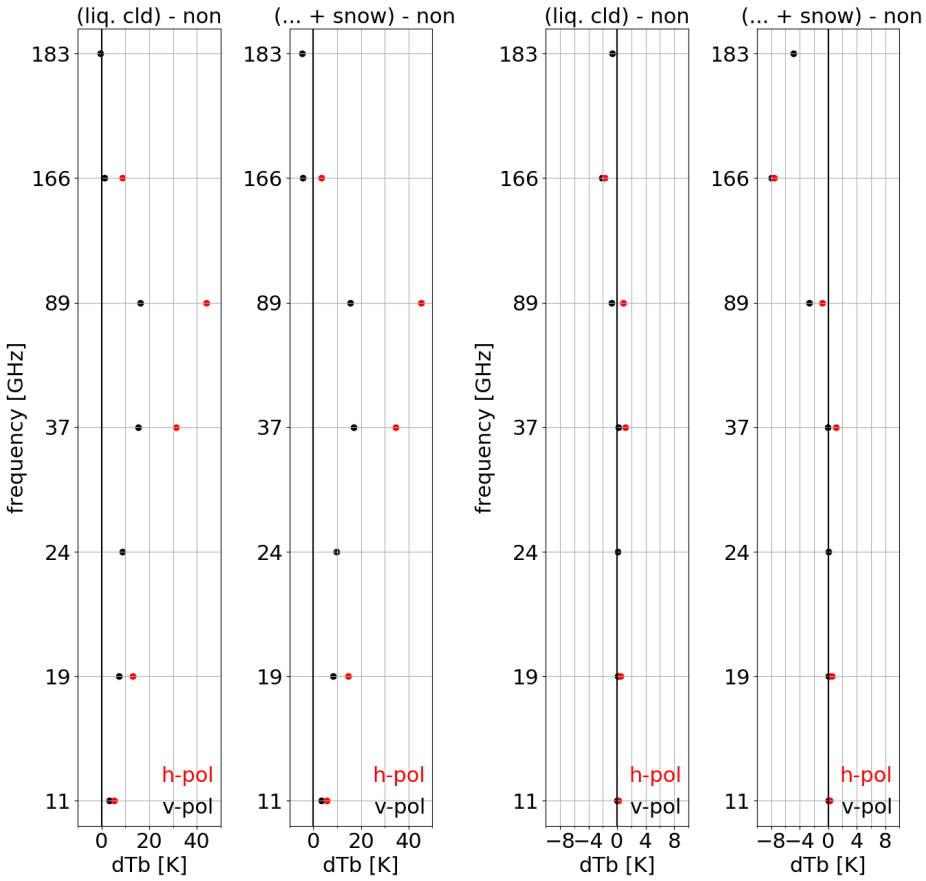

(a) Ocean surface, addition of liquid cloud water

(b) Ocean, addition of all hydrometeors

(c) Forest, addition of liquid cloud water

(d) Forest, addition of all hydrometeors

Figure 3: Difference in brightness temperatures for each GMI-like channel between a cloudy/precipitating atmospheric profile and a clear sky one. a) & c) show the differences using an atmospheric profile with just cloud liquid water added. b) & d) show the differences using an atmospheric profile with cloud liquid water, rain, cloud ice and snow. a) & b) correspond to conditions over ocean, whereas c) & d) correspond to conditions over forest. Note: x-axis has different scales for a) and b) compared to c) and d).

3 Experiments and the importance of land surface emissivity

The assimilation of microwave frequencies sensitive to humidity over land at 89/92 GHz and 150 /166 GHz in all-sky conditions has not been done before at ECMWF. Table 1 gives an overview of microwave frequencies which are sensitive to humidity from different instruments assimilated in the IFS over different surfaces. As shown, high-peaking humidity sounding channels at 183 GHz are used over all surfaces with some orography screening in place [Bormann et al., 2017, Weston et al., 2017], whereas most of

Table 1: Overview of the assimilation of brightness temperature at different microwave frequencies and polarisation (h=horizontally polarised, v=vertically polarised) which are sensitive to humidity over different surfaces in all-sky conditions in the IFS cycle 46R1. Frequencies between 19-89 GHz and 183 ± 4.5 & 7 GHz are assimilated between 60°N and 60°N, 150/166 GHz are assimilated between 45°N and 45°S. The remaining channels are assimilated globally. Coloured dots refer to brightness temperatures assimilated over ocean, snow-free land, sea-ice or snow-covered land. Filled dots refer to brightness temperatures which are assimilated operationally as of 4 June 2020, and unfilled dots refer to the brightness temperatures which are anticipated to be included into the all-sky assimilation in this study.

frequency [GHz], polarisation	GMI (GPM)	SSMIS-F17	SSMIS-F18	AMSR2 (GCOM-W)	MWRI (FY3D)	MWHS-2 (FY3C,D)	MHS (NOAA-18,19, Metop-A,B,C)
19v	●	●		●	●		
19h	●	●		●	●		
22/ 24v	●	●		●	●		
22/ 24h				●	●		
37v	●	●		●	●		
89/ 92v	●○	●○		●	●		
119 ±2.5h						●	
119 ±1.1h						●●	
119 ±0.8h						●●	
119 ±0.3h						●	
119 ±0.2h						●	
119 ±0.08h						●	
150/ 166v	●○						
150/ 166h	●○	●○					
183 ±7v/ h	●○	●●	●			●●	●●
183 ±4.5v						●●	
183 ±3v/ h	●○	●●●●	●			●●●●	●●●●
183 ±1.8v						●●●●	
183 ±1v/ h		●●●●	●			●●●●	●●●●

the remaining channels, and in particular the microwave window channels, are used over ocean. In this study, we test the addition of 89/92 GHz and 150 /166 GHz in all-sky conditions over land from GMI and SSMIS-F17 including the addition of 183 GHz channels from GMI over land. 89/92 GHz from AMSR2 and MWRI could not be tested as the assimilation over land uses an observation error model based on 150 GHz, which does not exist for those two instruments. In Geer et al. [2022] this issue has been addressed by using an updated observation error model.

3.1 Dynamic Emissivity Retrieval

In order to assimilate microwave brightness temperatures over land it is important to have a good knowledge of the surface emissivity because the atmospheric signals are much smaller, as illustrated in Fig. 3. This can be seen in the simplified radiative transfer equation assuming specular reflection and a non-scattering atmosphere:

$$T_b = T_{up} + T_{down}(1-\varepsilon)\tau + \tau\varepsilon T_s, \tag{1}$$

with the brightness temperature received at the satellite instrument, T_b, the atmospheric transmittance, τ, the surface emissivity, ε, the atmospheric up-welling brightness temperature T_{up}, the atmospheric down-welling temperature T_{down} and the skin temperature T_s.

In the dynamic emissivity retrieval, a certain surface emissivity is retrieved from satellite observations in a (different) selected surface-sensitive channel. The radiative transfer equation is solved for the surface emissivity and the remaining terms are estimated by using atmospheric profiles and skin temperature from the model background following the same principle, as done in former studies [Krzeminski et al., 2009, Karbou et al., 2010b,a]. A simplified version under clear sky conditions is

$$\varepsilon = \frac{T_b^{obs} - (\tau T_{down} + T_{up})}{(T_s - T_{down})\tau}. \tag{2}$$

This emissivity retrieval is also applied over sea-ice and snow-covered land but using a different surface-sensitive channel, meaning for the assimilation of 183 GHz channels over land we take 89/92 GHz, and over sea-ice and snow we take 150 GHz. By assuming that the spectral variability of emissivity is minimal, the retrieved surface emissivity is then used in the radiative transfer calculations of the specific channel, which is assimilated over land. If the dynamic retrieval exceeds expected bounds (deviates too highly from climatology or outside range 0-1), the atlas values (section 3.2) are used instead.

The all-sky assimilation over land uses the all-sky dynamic surface emissivity retrieval, described in Baordo and Geer [2016]. It differs from the clear-sky retrieval [Karbou et al., 2006] as it simultaneously retrieves the surface emissivity from within the clear sub-column and cloudy sub-column of RTTOV-SCATT, see equation (7) in Baordo and Geer [2016]. At the moment this approach is used for the humidity sensitive channels 119 GHz and 183 GHz from SSMIS-F17, MHS and MWHS-2, listed in Table 1. As previously mentioned, for the emissivity retrieval the 89/ 92 GHz channel is used over snow-free land and the 150/157 GHz channel is used over snow-covered land.

In this study, we tested the extension of the standard dynamic emissivity retrieval to the all-sky assimilation over land of 183 GHz channels of GMI, and 89/ 92 GHz and 150/166 GHz of GMI and SSMIS-F17. For these tests we used 91 GHz as the dynamic emissivity retrieval channel for the 183 GHz and 150/166 GHz channels and we used 37 GHz to provide the emissivity for the 89/ 92 GHz channels (making sure to use the retrieval from the appropriate polarisation in all cases). As discussed in Baordo and Geer [2016], the dynamical emissivity retrieval works well for allowing a successful assimilation over land of 183 GHz, and subsequently 119 GHz channels [Lawrence et al., 2018]. However, it has not yet been tested at any other frequencies. Also, in moderate to high cloud conditions the surface emissivity retrieval fails as the all-sky brightness temperatures of the window channel used in the retrieval contains a too large cloud signal. Baordo and Geer [2016] found that around 10% of observation over land would be too cloudy for the all-sky dynamic emissivity retrieval.

3.2 Emissivity Atlas

Another option to obtain emissivity is to use an emissivity atlas, as e.g. the Tool to Estimate Land Surface Emissivities at Microwave (TELSEM) atlas. This atlas is based on a pre-calculated monthly-mean emissivity climatology derived from 10 years of SSMI observations [Aires et al., 2011]. Within RTTOV, TELSEM provides monthly emissivity estimated for all land surfaces between 19 and 100 GHz and for all angles and linear polarisations. Here, clear-sky conditions have been selected to estimate surface emissivities, which makes the estimates reliable even when used in the all-sky assimilation of very cloudy conditions. However, due to changes in the soil moisture or land use the actual surface emissivity can vary from day to day. Hence we would like to find a way to represent this.

3.3 Spectrally Adjusted Emissivity Retrieval

In this approach we aim to combine the benefits of a dynamic surface emissivity retrieval with information on the frequency-dependence from an emissivity atlas. This is termed a spectrally adjusted emissivity retrieval. As a first step this uses a dynamic emissivity retrieval (section 3.1) at 19 GHz, vertically polarised (19 v GHz). Here, 19 GHz refers to either 18.7 GHz (GMI) or 19.35 GHz (SSMIS). This frequency is less sensitive to hydrometeors compared to higher frequencies (e.g. 89 GHz or 166 GHz) so it can be used to observe the land surface under almost all cloud conditions. In a second step the retrieved emissivity is adjusted using the relationship of emissivity with frequency known from the emissivity atlas. The frequency-emissivity relationship is taken from TELSEM, based on cloud-free conditions.

Figure 4 illustrates the idea behind the spectrally adjusted emissivity retrieval for clear and cloudy samples over the Amazon in June 2018. To identify cloudy and precipitating regions over land, the symmetric scattering index (SI) is used [Baordo and Geer, 2016]. The scattering index is the difference in brightness temperature between 91 h GHz and 150 h GHz, which can be computed from observations and first guess. The symmetric scattering index is the mean of both. For clear-sky and less cloudy/precipitating conditions, SI is low (smaller than -5) and for very cloudy/precipitating conditions SI is high (larger than 5) due to scattering from snow and ice hydrometeors. In mostly clear-sky conditions, the median retrieved emissivity (black line) slightly decreases with frequency, as seen in Fig. 4a. However, in very cloudy and precipitating conditions (Fig. 4b) the median retrieved emissivity follows a similar decrease towards 89 GHz but then drops to low values. This is because the magnitude of scattering increases at higher frequencies, leading to unphysical estimates of emissivity.

As mentioned before, in these conditions the use of an emissivity atlas helps. In Fig. 4 the emissivity atlas values (red line) do not show the sharp decrease in emissivity with frequency at high frequencies (Fig. 4b). In fact, the values slightly increase with frequency for both clear and cloudy conditions above 37 GHz. Even though the atlas emissivity estimates are better than the retrieval in very cloudy conditions, they are based on a monthly climatology. Hence the spectrally adjusted emissivity retrieval uses the advantage of the dynamical retrieval at 19 v GHz and then corrects this estimate to the emissivity value it should have at a particular frequency using the frequency dependence of the atlas (purple lines in Fig. 4). Using this approach, the variability of surface emissivity from the dynamical retrieval is preserved, but with a smaller chance of inducing errors due to the presence of clouds.

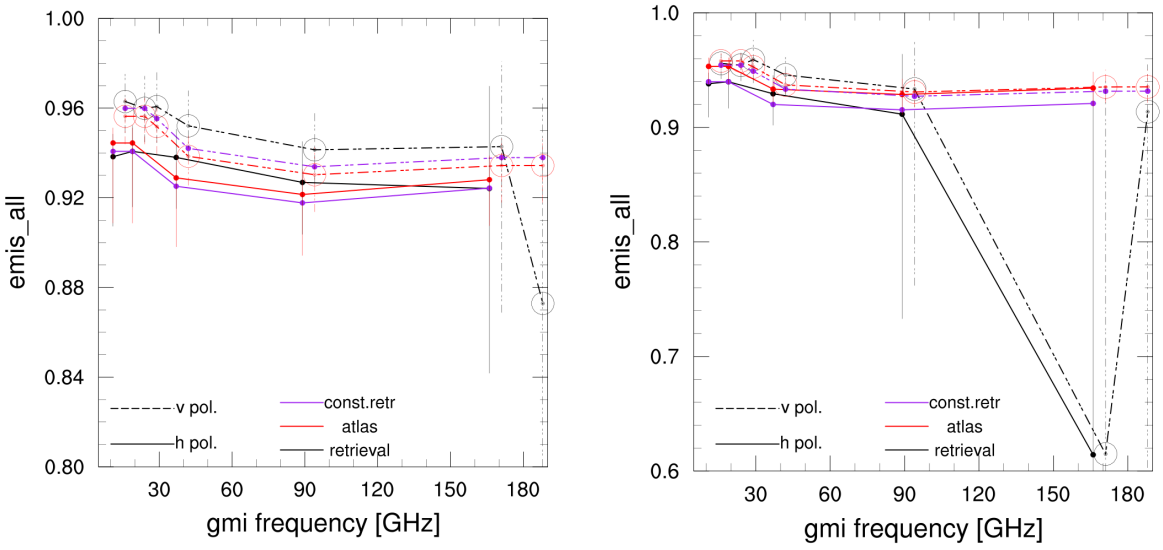

(a) Low SI

(b) High SI

Figure 4: Emissivity as function of frequency [GHz] taken from GMI observations in June 2018 over (snow-free) land in the Amazon (20°S-10°N, 40°W-80°W) with a) symmetric scattering index (SI) of -5 and lower and with b) SI larger than 5. Solid horizontal lines refer to horizontally polarised channels, and dashed horizontal lines to vertically polarised ones. Black: dynamic emissivity retrieval, red: TELSEM atlas and purple: spectrally adjusted emissivity retrieval lines. The dots refer to the median in emissivity at a certain frequency with the vertical lines showing the range between the 5^{th} and the 95^{th} percentile. The median emissivity of the vertically polarised channels are plotted with an offset of 5 GHz.

3.4 Experimental setup

To investigate the effect of using different estimates of surface emissivity in the additional assimilation of channels at 89 GHz and higher over land, we have set up various 46R1 experiments at TCo399 horizontal resolution. Here, it is important to mention that the spectrally adjusted emissivity retrieval is only applied to vertically polarised channels. In Fig. 4a it can be seen that the emissivity varies differently with frequency for the horizontally polarised channels than for the vertically polarised ones. The frequency variation is different between the atlas and the dynamic emissivity retrievals, and the origin of this behaviour is not clear. To exclude any induced errors originating from this behaviour we choose to apply the spectrally adjusted retrieval only to vertically polarised channels. In any case, mid-frequency horizontally polarised channels are not part of the assimilation of surface sensitive microwave channels over ocean either.

We have set up experiments assimilating additional channels over land from GMI and SSMIS observations. The experiments are run for a summer (June-August 2018) and a winter season (November 2018 - February 2019), excluding the first month in the analysis to avoid spin-up issues. Here, data over snow and at high latitudes (north of 60°N and south of 60°S) are excluded. After testing the different flavours of emissivity estimates in the additional land assimilation using GMI observations (GMI_{base}) the role of bias correction (section 4.2) has been investigated. For this reason, additional experiments (GMI_{newBC}) have been set up. Finally, a configuration using the spectrally adjusted emissivity retrieval for GMI and

Table 2: Overview of GMI_{base} 46R1 experiments testing the additional all-sky assimilation over land run for a summer (June-August 2018) and a winter season (November 2018 - February 2019).

surface emissivity estimate	GMI_{base}
retrieval	GMI_{ret}
atlas	GMI_{atl}
spectrally adjusted retrieval	GMI_{adj}
control (no additional land assimilation)	CTL

SSMIS using a new version of bias correction is tested.

4 Results

4.1 Verification of GMI_{base} experiments

Table 2 gives an overview of the different GMI_{base} experiments, which additionally assimilate GMI channels 89 v GHz, 166 v,h GHz, $183 \pm 7{,}3$ v GHz over land (GMI_{ret}, GMI_{atl} and GMI_{adj}), and a control run (CTL). When using the spectrally adjusted emissivity retrieval (GMI_{adj}) only the vertically polarised channels (89 v GHz, 166 v GHz, $183 \pm 7{,}3$ v GHz for GMI) use the spectrally adjusted emissivity approach (section 3.3), whereas the horizontally polarised channels (166 h GHz for GMI) use the dynamic emissivity retrieval (section 3.1).

4.1.1 Observational verification

To verify the GMI_{base} experiments for the short-range forecast, fits to other independent observations are checked. Observational fits which are sensitive to humidity and temperature, like the Advanced Microwave Sounding Unit-A (AMSU-A, from Aqua, NOAA-15, NOAA-16, NOAA-18, NOAA-19, Metop-A and Metop-B; Fig.5b) or the Advanced Technology Microwave Sounder (ATMS, from NPP) show a mostly neutral effect using all three emissivity estimates, with GMI_{adj} having slightly improved fits to channels 10 to 12. Wind observations from Atmospheric Motion Vectors (AMVs; Fig.5d) and wind profiles, and clear sky radiances (Fig.5a) show a neutral effect, too. Fits to Meteosat-11 for the water vapour channel 7.3μm show an improved fit for GMI_{adj} and GMI_{atl}. Some water vapour sensitive channels of CRIS (Fig.5c) show a small but insignificant improvement for all emissivity estimates. For most surface sensitive observations the addition of GMI observations over land has a neutral impact except for relative humidity where a small significant improvement can bee seen as shown in Fig.5e. For radiosonde temperature observations (Fig.5f) only GMI_{adj} gives a neutral impact for all height levels. In summary, fits to independent observations are mostly neutral with GMI_{adj} showing slightly better fits.

4.1.2 Forecast scores

To study how global forecast scores are affected we look at the change in the root-mean-square of forecast error (RMSE) of different variables. A decrease in RMSE would usually be interpreted as an improve-

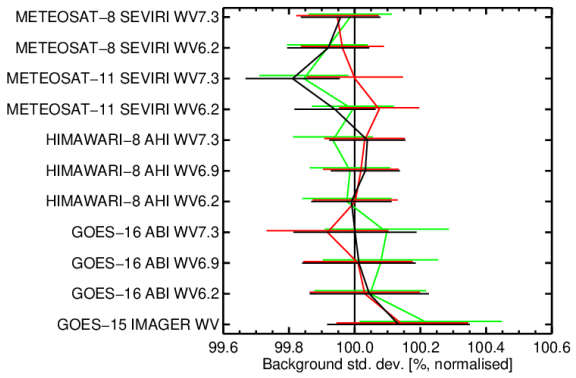

(a) Clear-sky radiance from geostationary satellites.

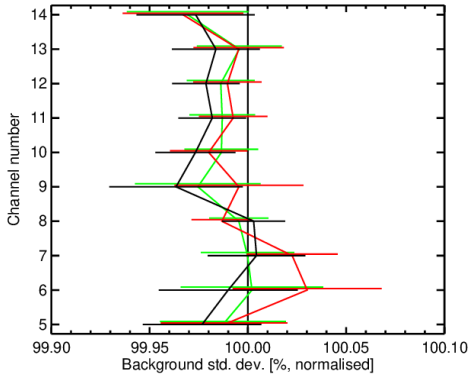

(b) AMSU-A

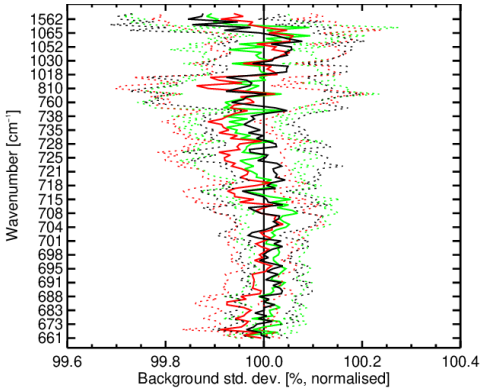

(c) CRIS

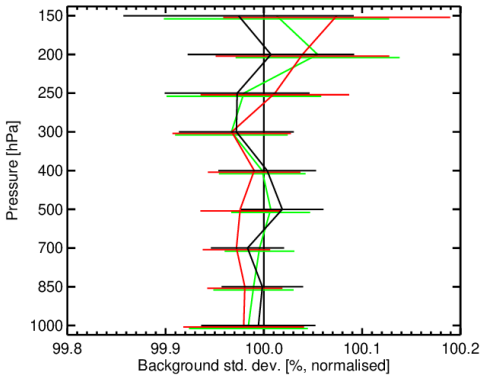

(d) Atmospheric Motion Vectors

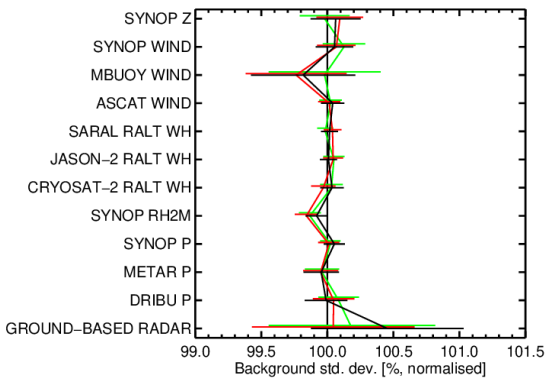

(e) Surface observations

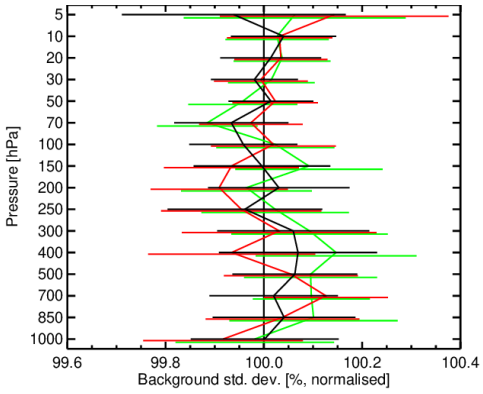

(f) Radiosonde temperature

Figure 5: Normalised standard deviation of first-guess departures from GMI_{atl}, GMI_{ret} and GMI_{adj} (black) for different instruments. The normalisation is done with results from CTL. Values less than 100% would indicate beneficial impacts from the experiments. The horizontal bars indicate 95% confidence range. Results cover the time period from 1 July to 31 August 2018 and 1 December 2018 to 28 February 2019.

ment and an increase in RMSE as a degradation in forecast scores. However, as shown later one has to be careful with this interpretation. Fig. 6 shows averages in normalised difference in RMSE in humidity

between the different GMI_{base} experiments and CTL for 1000 hPa and 850 Pa and for different latitude bands. For the southern and northern hemisphere all emissivity estimates show neutral RMSEs in humidity in the lower troposphere throughout the forecast. In the tropics, some apparent degradations for GMI_{adj} and some apparent improvements for GMI_{ret} are visible up to forecast day 4. However, no such signals have been found in fits to independent humidity sensitive observations in these areas. Additionally, no changes in RMSE are seen for humidity in the mid- or high atmosphere and for temperature and wind.

To investigate the humidity signal in the forecast scores in more detail, we look at the mean difference in near-surface (1000 hPa) analysis humidity for all GMI_{base} experiments, as shown in Fig. 7. It is interesting to see that the different emissivity estimates have different effects on the analysis. The drying signal over Africa for GMI_{ret} (Fig. 7a) and GMI_{atl} (Fig. 7b), might be explained by challenges in capturing the correct diurnal cycle in the surface temperature estimate used in the radiative transfer calculations in desert regions [Bormann et al., 2017]. However, changes of surface humidity over ocean for GMI_{ret} (Fig. 7a, moistening) and GMI_{adj} (Fig. 7c, drying) seem peculiar, as these experiments have only added the assimilation of selected microwave frequencies over land. Interestingly, in GMI_{ret}, the tropical moistening at 1000 hPa over ocean is associated with a decrease in RMSE in humidity, whereas for GMI_{adj}, the tropical drying signal at 1000 hPa over ocean is associated with an increase in RMSE in humidity (see Fig. 6). It is only the mean error in humidity that has changed in the tropical lower atmosphere (and not the standard deviation, not shown) with a decrease for GMI_{ret} and an increase for GMI_{adj} up to forecast day 4.

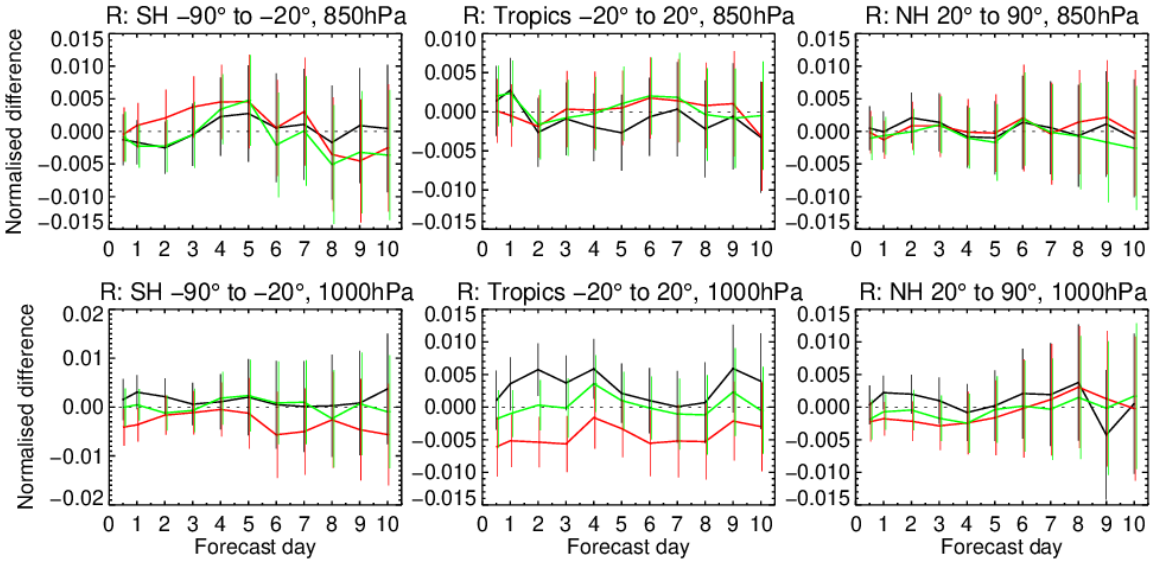

Figure 6: Averages of differences in RMSE in humidity between GMI_{atl}, GMI_{ret} and GMI_{adj} (black) experiments, and CTL, verified against own analysis at different height levels (1000 hPa and 850 hPa) for different forecast times and zonal regions. Negative values represent a decrease in RMSE and positive values an increase in RMSE for GMI_{base} experiments. Results cover the time period from 1 July to 31 August 2018 and 1 December 2018 to 28 February 2019. The confidence range is displayed by vertical bars.

Table 3: Overview of GMI_{noBC} 46R1 experiments testing the additional all-sky assimilation over land without using bias-corrected brightness temperatures in the emissivity retrieval, run for a summer (June-August 2018) and a winter season (November 2018 - February 2019).

surface emissivity estimate	GMI_{noBC}
retrieval	GMI^{ret}_{noBC}
spectrally adjusted retrieval	GMI^{adj}_{noBC}

4.2 Role of bias correction

The absolute mean change in analysis surface humidity over the tropical ocean is largest for GMI_{ret} (about 0.2%, Fig. 7a) and smaller for GMI_{adj} (about 0.1%, Fig. 7c). Even though these mean changes in humidity do not appear to be big, it is a systematic feature which needs to be investigated. We think that this behaviour must be linked to the bias correction in two different ways. The first one is thought to be linked to using bias-corrected brightness temperatures in the emissivity retrievals. This is supported by the results of GMI_{atl}, which does not need to calculate emissivity values using brightness temperatures, and which does not show any moistening or drying effect over ocean (Fig. 7b). For the other two experiments, bias corrected brightness temperatures are used in the dynamic emissivity retrieval. Hence, we have set up additional experiments for GMI_{ret} and GMI_{adj} to test using non bias-corrected brightness temperatures, see Table 3. As shown in Fig. 8b, when using non bias-corrected brightness temperatures in the emissivity retrieval, the drying over ocean for GMI_{adj} vanishes. However, the moistening over the tropical ocean is still apparent for GMI_{ret} (Fig. 8a).

That means there must be another way that bias correction affects the mean analysis of surface humidity over ocean, when the emissivity retrieval approach is used for many different microwave radiances over land. To get a better understanding how bias correction changes in GMI_{ret}, the relative change in bias

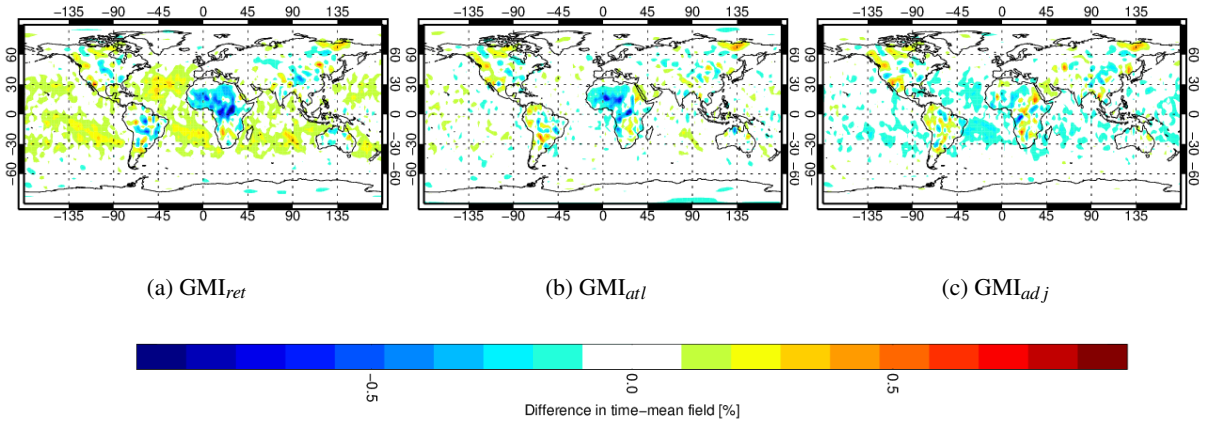

(a) GMI_{ret} (b) GMI_{atl} (c) GMI_{adj}

Figure 7: Difference in analysis humidity between the different GMI_{base} experiments and CTL at 1000 hPa with a) GMI_{ret}, b) GMI_{atl} and c) GMI_{adj}. Results cover the time period from 11 July to 31 August 2018 and 11 December 2018 to 28 February 2019.

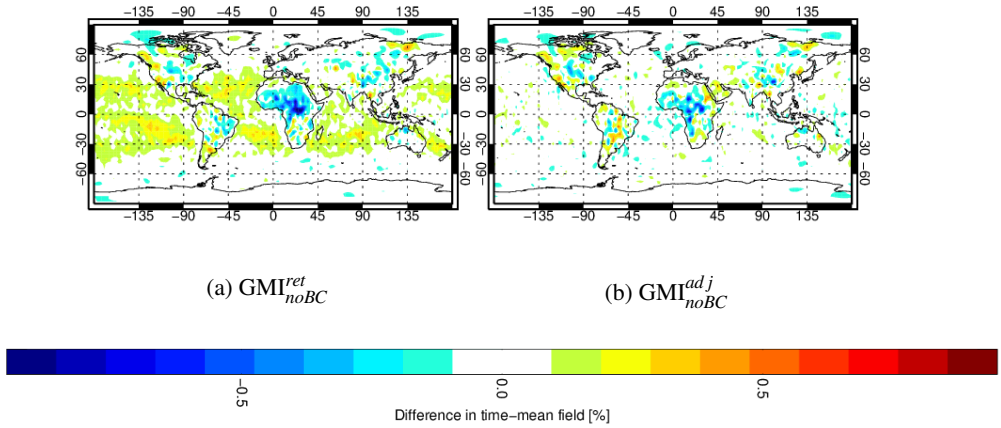

(a) GMI^{ret}_{noBC} (b) GMI^{adj}_{noBC}

Figure 8: Difference in analysis humidity between the different a) GMI^{ret}_{noBC} and b) GMI^{adj}_{noBC}, and CTL at 1000 hPa. In both experiments no bias correction is applied to the brightness temperatures in the emissivity retrieval. Results cover the time period from 11 July to 31 August 2018 and 11 December 2018 to 28 February 2019.

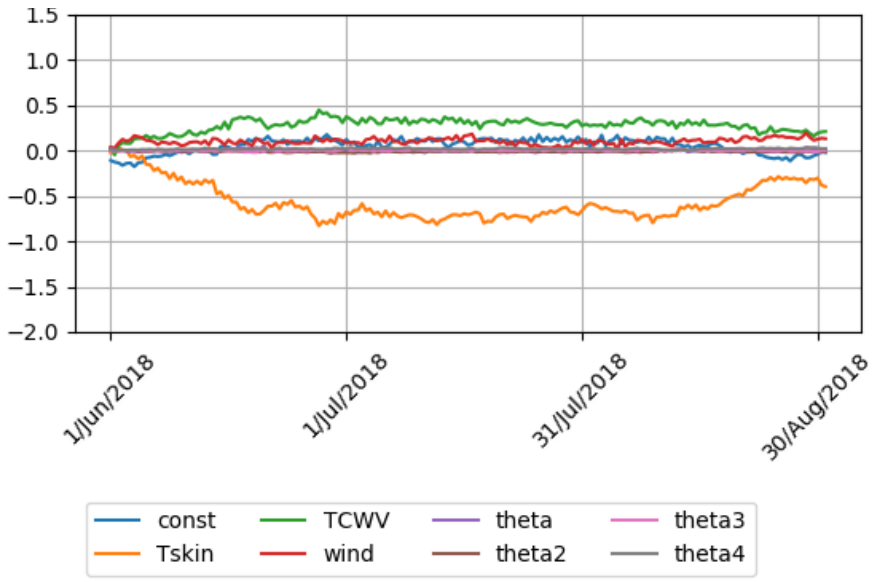

Figure 9: Difference in predictor coefficients at 89 v GHz from GMI between GMI_{ret} and CTL as a function of assimilation time. Results cover the time period from 1 June to 31 August 2018.

predictors for this experiment are plotted for 89 v GHz as a function of assimilation time in Fig. 9. It is only at this frequency that significant differences between in the bias predictors could be seen, and these differences are limited to the skin temperature predictor. The skin temperature, T_{skin}, was identified by Harris and Kelly [2001] as a good bias predictor for the assimilation of microwave frequencies. Hence it is used for all surface sensitive microwave channels in the Integrated Forecast System (IFS). For higher microwave frequencies (e.g. 166 GHz or 183 GHz) the bias predictors do not include skin temperature because those channels are less sensitive to the surface. In the study by Harris and Kelly [2001] the

T_{skin} predictor was only tested for the assimilation of microwave observations over ocean. We know that the dependence of bias on T_{skin} over ocean is different from the dependence over land, so it might be questionable to use T_{skin} as a bias predictor over both land **and** ocean. This is supported by the changes when used in the assimilation over land based on emissivity retrievals (Fig. 9). The coefficient for the T_{skin} bias predictor is reduced in GMI_{ret} compared to CTL, and hence is likely linked with the corresponding moistening over tropical ocean.

To further investigate the results of using T_{skin} as a bias predictor over ocean and land for GMI_{ret}, we test if there is still a residual bias. This is checked by showing the FG departure after bias correction as a function of T_{skin} (Fig. 10). For ocean we see little residual bias for most skin temperatures, which means the bias correction works well. However, for land the residual bias is about -3 K for most skin temperatures. For GMI_{adj} we find a similar behaviour with almost no residual bias over ocean, but a residual bias of 1 K to 2 K over land (not shown). This shows that T_{skin} is not able to simultaneously predict the bias over ocean and land. It might be better to use a new bias predictor for surface sensitive microwave channels when they are assimilated over both land and ocean. We found that the behaviour of the bias predictor T_{skin} only changes for 89/92 v GHz (Fig. 9) so we are only interested in finding an alternative bias predictor for this channel. A study by Gerard et al. [2011] suggests using $T_{skin}\varepsilon_{19v}$ with ε_{19v} the emissivity at 19 v GHz, as a bias predictor for microwave frequencies assimilated over land and ocean. This predictor enables a distinction between land and sea, and corresponds to the surface contribution of radiation. Gerard et al. [2011] found $T_{skin}\varepsilon_{19v}$ was a better discriminator between land and sea by taking into account some variability over land than a standard land-sea mask only distinguishing between land and ocean.

As described in section 3, GMI_{newBC} experiments have been set up to test the use of the new bias predictor instead of T_{skin} for 89 v GHz. Table 4 lists the different GMI_{newBC} experiments. Figure 11a displays

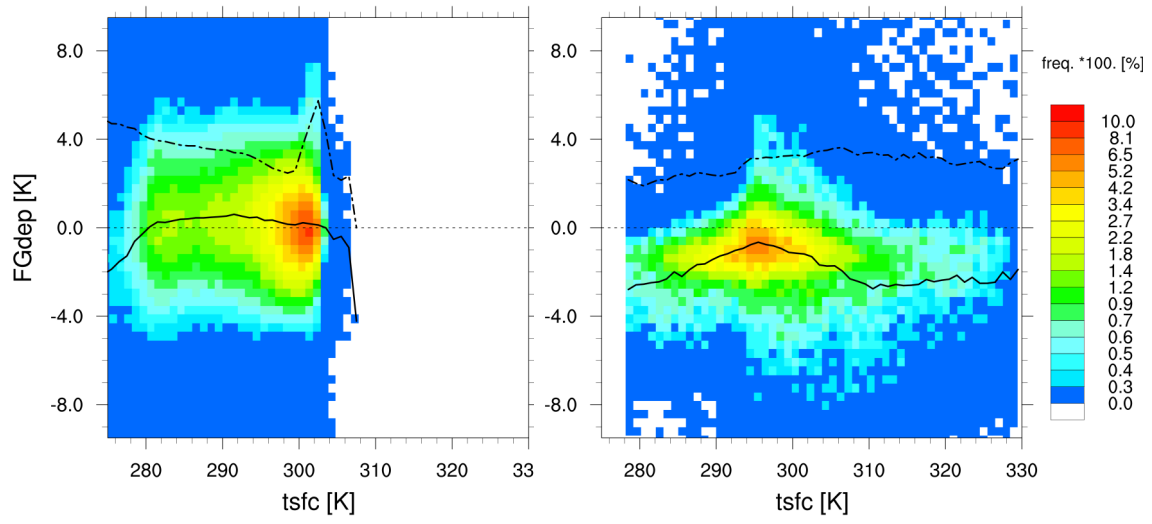

(a) Ocean

(b) Land

Figure 10: Residual bias (FG departure) as a function of skin temperature (tsfc) for GMI observations at 89 v GHz for GMI_{ret} over a) ocean and b) land. The colours show the number of observations, the solid black line the mean and the dashed line the standard deviation.

Table 4: Overview of GMI_{newBC} 46R1 experiments testing the additional all-sky assimilation over land with a new bias correction for 89 v GHz, run for a summer (June-August 2018) and a winter season (November 2018 - February 2019).

surface emissivity estimate	GMI_{newBC}
retrieval	GMI^{ret}_{newBC}
spectrally adjusted retrieval	GMI^{adj}_{newBC}

the change in RMSE for surface humidity in the tropics for GMI_{newBC}. Here, both experiments show a slight decrease in RMSE. This apparent improvement must be linked to the use of the new bias predictor for 89 v GHz. An experiment applying the new bias correction to 89 v GHz without the additional assimilation of more microwave frequencies over land shows the same behaviour, as demonstrated in Fig. 11b. The usage of the new bias correction results in the analysis near the ocean surface being moistened in the tropics and dried outside of the tropics compared to CTL. This can be seen for the ocean only experiment (Fig. 12c) and all the GMI_{newBC} experiments (Fig. 12a and Fig. 12b) using the new bias predictor.

4.3 Final configuration

In light of findings from previous sections (in particular, section 4.2), it was decided to test a final pair of experiments. These experiments assimilate microwave frequencies of 89/92 v GHz and higher over land from GMI and SSMIS-F17 using the spectrally adjusted retrieval approach. The performance in terms of short-range forecast impact evaluated against observations is in line with results from the GMI^{adj}_{newBC} experiment, with some minor strengthening of the signal (cf Fig. 5 and Fig. 13). Furthermore, the temperature, humidity and wind forecast scores are mostly neutral. The typical decrease in RMSE

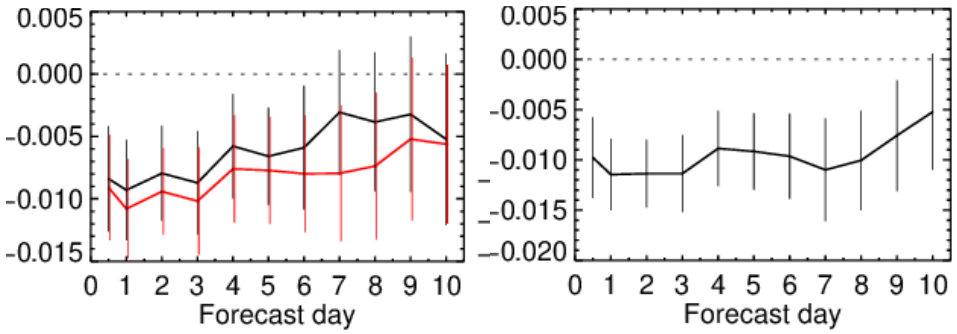

(a) GMI_{newBC} experiments.

(b) Ocean only experiment using new bias predictor for 89 v GHz.

Figure 11: Same as Fig. 6 just showing averages of differences in RMSE in humidity between a) GMI_{newBC} experiments or b) ocean only experiment using new bias predictor for 89 v GHz, and CTL normalised by CTL. For a) red line corresponds to GMI^{ret}_{newBC} and black line to GMI^{adj}_{newBC}. Verification is done against own analysis at 1000 hPa for different forecast times in the Tropics (20°S-20°N).

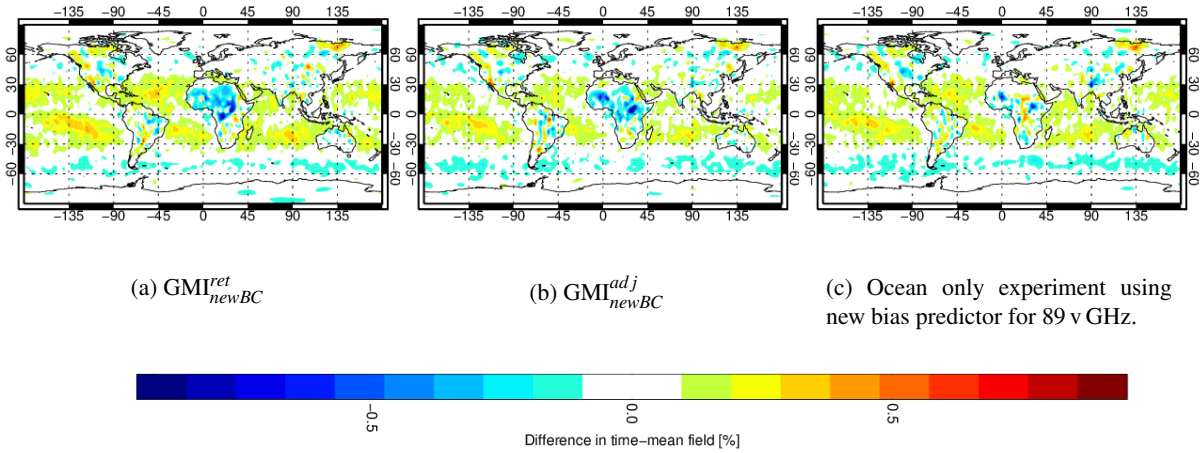

(a) GMI^{ret}_{newBC} (b) GMI^{adj}_{newBC} (c) Ocean only experiment using new bias predictor for 89 v GHz.

Figure 12: Difference in analysis humidity between a) GMI^{ret}_{newBC}, b) GMI^{adj}_{newBC} and c) ocean only experiment using new bias predictor for 89 v GHz, and CTL at 1000 hPa. Results cover the time period from 11 July to 31 August 2018 and 11 December 2018 to 28 February 2019.

in surface humidity in the tropics can be found (not shown), which comes along with a moistening of the analysis at 1000 hPa in the tropics and a drying outside of the tropics (not shown). As discussed in section 4.2, this is due to the new bias correction at 89/92 v GHz.

In summary, the results demonstrate that microwave window channels can be usefully assimilated over land in an all-sky approach. While the forecast impact is relatively small, it is overall in line with expectations given smaller cloud signals found over land than over ocean in our off-line experimentation (section 2).

4.4 Limitations

One feature seen in Fig. 12b and Fig. 12a has not been discussed yet, which is the drying of the analysis in the lower troposphere over the Sahara, when assimilating microwave observations over land. This drying looks similar to Fig. 16 of Weston et al. [2019]. They argue that these changes in mean analysis are related to diurnal biases in surface sensitive microwave channels over arid regions caused by the neglect of penetration effects that is implicit in the use of the model skin temperature in the dynamic emissivity retrieval [Bormann et al., 2017]. In GMI_{newBC}, surface sensitive channels are assimilated over land for the first time, but no adequate quality control or sink variable is in place which would remove bias-affected brightness temperatures. Geer et al. [2022] subsequently identified that the spectrally adjusted emissivity retrieval is not appropriate for scenes such as these, with internal ("volume") scattering of microwave radiation, such as deserts, dry soils, snow and ice. Hence, they introduced a new quality check based on the polarisation difference at 37 GHz and on a surface type estimation using the 19v - 89v differences. Another study by Weston et al. [2019] suggests introducing the skin temperature as a sink variable, along with developing a quality control to reject observations when the diurnal bias is too strong.

Another aim which was not achieved in this study was the additional assimilation of 89/92 v GHz from MWRI and AMSR2 over land. This was not possible because the observation error model used in

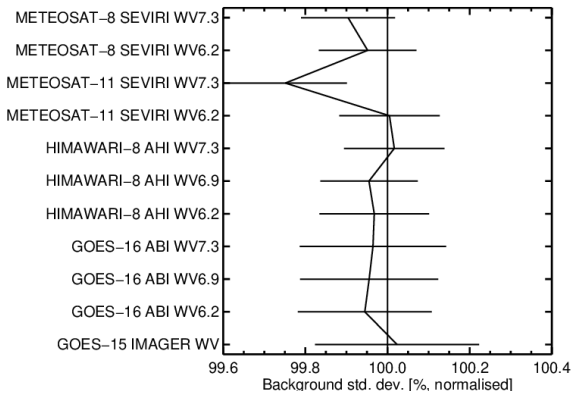

(a) Clear-sky radiance from geostationary satellites.

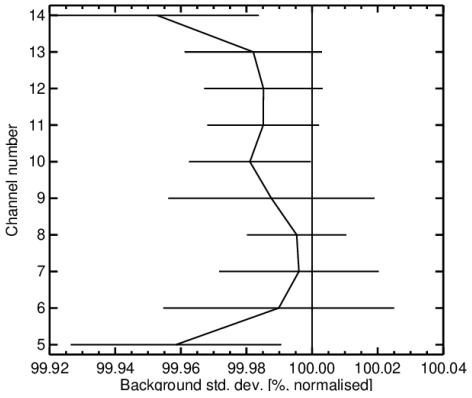

(b) AMSU-A

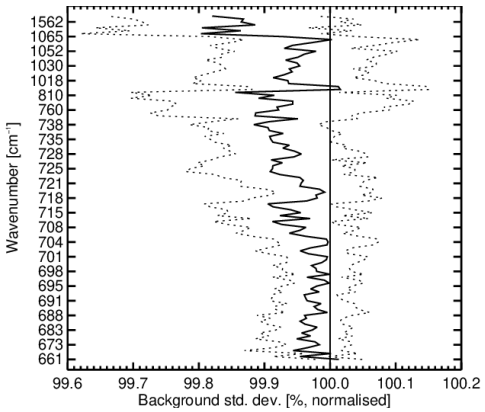

(c) CRIS

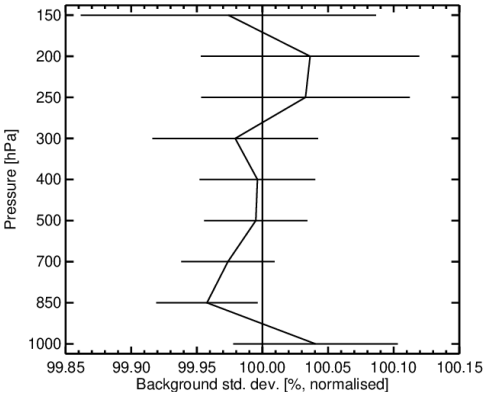

(d) Atmospheric Motion Vectors

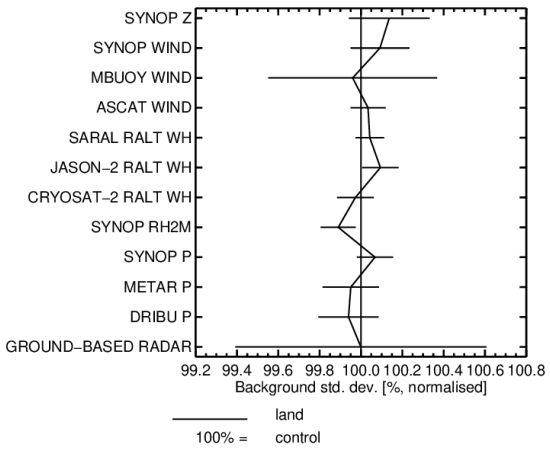

(e) Surface observations

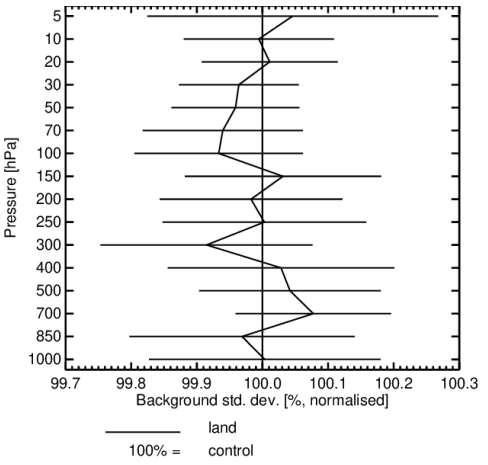

(f) Radiosonde temperature

Figure 13: Normalised standard deviation of first-guess departures in SSMIS-GMI$^{adj}_{newBC}$ for different instruments. The normalisation is done with results from CTL. Values less than 100% would indicate beneficial impacts from the experiments. The horizontal bars indicate 95% confidence range. Results cover the time period from 1 July to 31 August 2018 and 1 December 2018 to 28 February 2019.

the present study relies on the 150/166 h GHz channel, but this is not present on these instruments. Active assimilation of these channels requires the development of a new observation error model. This has subsequently been done by [Geer et al., 2022] for window channels 37 v GHz and 89 v GHz for all microwave imagers over land, using a constant value for observation error to minimise the impact of surface-related errors due to skin temperature, volume scattering, etc.

Lastly, it is worth mentioning that there is a limitation to any non-dynamic or non-physically modelled emissivity, like the atlas or the spectrally adjusted emissivity retrieval. This is because we assume that the spectral characteristics of emissivity do not vary within a month, as it is based on the monthly atlas values. Land surface emissivity depends largely on soil type, soil wetness and vegetation [Petty, 2006]. If the surface is heavily flooded the spectral dependence of emissivity looks quite different compared to dry land. This does not pose an issue if it is captured by the monthly climatology but would be if it is not. However, the aim for using a spectrally adjusted emissivity retrieval is to avoid situations where we have to use atlas emissivity values instead of real time retrievals in very cloudy situations. In these situations we believe that using the adjusted retrieval is superior to the atlas approach as it is capturing part of the instantaneous variations. To improve it even further, the usage of a different climatology (maybe based on daily variations) would help better capture variations in the spectral characteristics of emissivity.

Also linked to this issue is the exclusion of the spectrally adjusted emissivity retrieval for horizontally polarised channels. As mentioned in section 3.4, there is more variability in the frequency dependence of emissivity than in the vertically polarised channels. This is shown by the longer vertical bars in Fig. 4. Prigent et al. [2000] have also shown how land emissivity at microwave frequencies in vertical and horizontal polarisation differs for various surfaces. Here, differences are largest for less vegetated areas (e.g. bare soil, see their Fig. 1) and when it is very dry (e.g. deserts, see their Fig. 2) in clear-sky conditions. However, differences are also present in crop fields, where geometrical effects can be significant. In cloudy conditions the horizontally polarised channels are more sensitive to hydrometeors than the vertically polarised ones. Hence, further sensitivity studies are necessary to evaluate how well the adjusted emissivity retrieval works over all surfaces during all-sky conditions for horizontally polarised channels.

5 Summary and Outlook

In this study we explore how to best assimilate surface-sensitive microwave frequencies over land using the all-sky approach. The challenge for those channels lies in the unsatisfactory knowledge of surface properties, for example skin temperature and surface emissivity, in the microwave spectrum for different surfaces ranging from deserts to tropical forests. Over ocean, the surface emissivity can be modelled using FASTEM, which currently cannot be done with satisfactory accuracy over land.

For now, we are only interested in the atmospheric signal of the all-sky brightness temperature in the assimilation of microwave frequencies - over all surfaces. For this reason, we have conducted an off-line analysis to check which frequencies have a big enough signal from hydrometeors over different land surfaces. It has been found that frequencies at 89/92 GHz and higher contain enough signal from the atmosphere to be distinguishable from the surface signal. Hence, this study concentrates on testing the all-sky assimilation over land of those frequencies. In the future, one should work on a coupled approach to assimilate surface-sensitive microwave brightness temperatures both to improve the initial conditions of the atmosphere, e.g. total water vapour, and of the surface, e.g. soil moisture. Until now, only satellite derived products have been used to improve land surface conditions, within a separate land analysis. Going in the direction of a coupled approach would allow the land assimilation of lower microwave frequencies to become an integral part of constraining surface properties.

To obtain a good estimate of the surface, a dynamic emissivity retrieval has been used for the all-sky assimilation of less surface-sensitive microwave channels over land. However, this study shows that using this approach for the assimilation of 89/ 92 GHz comes along with a moistening over the tropical ocean through an interaction with bias correction. We have tested a spectrally adjusted emissivity retrieval, which retrieves emissivity at 19 v GHz and then adjusts this value using the dependency of emissivity with frequency obtained from TELSEM atlas. The big advantage of a spectrally adjusted emissivity retrieval is that it can be used in all cloud conditions. For example, in very cloudy conditions the standard dynamic emissivity retrieval fails and the emissivity estimate from TELSEM is used instead. The spectrally adjusted emissivity retrieval is only used for vertically polarised channels in this study as the sensitivity to clouds and water vapour is different for horizontally polarised channels, which can be seen e.g. by a different variation of emissivity with frequency. However, the spectrally adjusted emissivity retrieval could still be extended to horizontally polarised channels using a retrieved emissivity at 19 h GHz instead, awaiting more testing.

A new bias predictor, skin temperature times emissivity at 19 v GHz, has been used for 89/ 92 v GHz in this study to better encapsulate the biases coming from land/ sea differences. However, this additional predictor led to changes in the applied bias correction over ocean as well as land, and changes in the forecast impact described in the next paragraph. To avoid changing the assimilation of observations over ocean as a side effect of adding them over land, in our subsequent study we tried a different bias correction approach. Geer et al. [2022] instead used two predictors, the land sea mask, and the land sea mask times the skin temperature, to allow the bias correction over land to be mostly independent from that over ocean. In more general terms, it might be necessary to reconsider the usage of the bias predictor T_{skin} and total column water vapour (TCWV) for surface sensitive microwave channels as it has never been explicitly studied how the introduction of the all-sky approach affects the necessity in using them - also over sea. In this study we only modified one bias predictor for one channel, and the impact was large. Hence it is important to further study the effect of removing some bias predictors for potentially all surface sensitive channels.

In this study we test the additional assimilation over land of 89/ 92 v GHz and 150/ 166 GHz from GMI and SSMIS-F17, and the 183 GHz channels from GMI using the spectrally adjusted emissivity retrieval and the new bias correction for 89/ 92 v GHz. Results from a combined summer and winter period show mostly neutral forecasts scores and neutral fits to independent observations with small improvements to AMVs at 850 hPa and clear sky radiances for Meteosat-11 at 7.3μm. These neutral to small improvements are as expected from running the off-line experiments. The largest change, however, is actually triggered by the usage of the new bias predictor for 89/ 92 v GHz. Here, the surface humidity over ocean is decreased at midlatitudes and increased over the tropical ocean, which results in a decrease in RMSE for near surface humidity in the Tropics. By using an alternative set of bias predictors based on the land-sea mask, Geer et al. [2022] were able to prevent such changes occurring. Another effect of the current setup of the land assimilation is a drying over the Sahara, which is most likely related to diurnal biases in the model skin temperature. We were able to subsequently address this in Geer et al. [2022] using a new quality check to prevent the assimilation of microwave window channels over such regions.

These assimilation results at 89/92 GHz (and higher) over land motivated us to investigate additional frequencies (e.g. 37 GHz) and additional sensors (e.g. AMSR2) in our subsequent work [Geer et al., 2022]. However, in order to do that, that study needed to find a new observation error model. This was because the current observation error model was mostly aimed at describing cloud related errors, whereas over land much of the error budget comes from errors in the surface description. In future, one might come up with an even more sophisticated error model over land based on emissivity or soil moisture as the microwave brightness temperatures over land are highly dominated by emissivity or skin temperature

errors. Furthermore, this study covers the additional assimilation over land, but leaves out the additional assimilation over sea ice and snow. Geer et al. [2022] addresses this for GMI 183+/-3 GHz channel over sea-ice using a standard dynamic emissivity approach, bringing the assimilation of microwave radiance closer to an "all-sky all-surface system".

Acknowledgements

Katrin Lonitz's work at ECMWF is funded by the EUMETSAT fellowship programme.

References

F. Aires, C. Prigent, F. Bernardo, C. Jimenez, R. Saunders, and P. Brunel. A Tool to Estimate Land-Surface Emissivities at Microwave frequencies (TELSEM) for use in numerical weather prediction. *Q. J. R. Meteorol. Soc.*, 137:690–699, 2011.

F. Baordo and A. J. Geer. Assimilation of SSMIS humidity-sounding channels in all-sky conditions over land using a dynamic emissivity retrieval. *Q. J. R. Meteorol. Soc.*, 142(700):2854–2866, 2016.

P. Bauer, A. J. Geer, P. Lopez, and D. Salmond. Direct 4D-Var assimilation of all-sky radiances: Part I. implementation. *Q. J. R. Meteorol. Soc.*, 136:1868—1885, 2010.

N. Bormann, C. Lupu, A. Geer, H. Lawrence, P. Weston, and S. English. Assessment of the forecast impact of surface-sensitive microwave radiances over land and sea-ice. Technical Memorandum 804, ECMWF, 2017.

S. English. The importance of accurate skin temperature in assimilating radiances from satellite sounding instruments. *IEEE Trans. Geosci. Remote Sens.*, 46:403–408, 2008.

S.J. English and T.J. Hewison. A fast generic microwave emissivity model. In Tadahiro Hayasaka, Dong Liang Wu, Yaqiu Jin, and JingShang Jiang, editors, *Microwave Remote Sensing of the Atmosphere and Environment*, number 3503, pages 288 – 300. International Society for Optics and Photonics, SPIE, 1998. doi: 10.1117/12.319490.

A. Geer, K. Lonitz, D. I. Duncan, and N. Bormann. Improved surface treatment for all-sky microwave observations. Technical Memorandum 894, ECMWF, 2022.

A. J. Geer and P. Bauer. Observation errors in all-sky data assimilation. *Q. J. R. Meteorol. Soc.*, 137: 2024—2037, 2011.

E. Gerard, F. Karbou, and F. Rabier. Potential use of surface-sensitive microwave observations over land in numerical weather prediction. *IEEE TRANSACTIONS ON GEOSCIENCE AND REMOTE SENSING*, 49(4):1251–1261, 2011.

B. A. Harris and G. Kelly. A satellite radiance-bias correction scheme for data assimilation. *Q. J. R. Meteorol. Soc.*, 127(574):1453–1468, 2001.

F. Karbou, E. Gerard, and F. Rabier. Microwave land emissivity and skin temperature for AMSUA and -B assimilation over land. *Q. J. R. Meteorol. Soc.*, 132:2333–2355, 2006.

F. Karbou, F. Rabier and. J.-P. Lafore, J.-L. Redelsperger, and O. Bock. Global 4d-var assimilation and forecast experiments using AMSU observations over land. Part II: impact of assimilating surface sensitive channels on the african monsoon during AMMA. *Weather and Forecasting*, 25:20–36, 2010a.

F. Karbou, E. Gerard, and F. Rabier. Global 4d-var assimilation and forecast experiments using AMSU observations over land. part-i: Impact of various land-surface emissivity parameterizations. *Weather and Forecasting*, 25:5–19, 2010b.

B. Krzeminski, N. Bormann, F. Karbou, and P. Bauer. Improved use of surface- sensitive microwave radiances over land at ecmwf. EUMETSAT Meteorological Satellite Conference, Darmstadt, Germany, EUMETSAT, 2009.

H. Lawrence, N. Bormann, A. J. Geer, Q. Lu, and S. J. English. Evaluation and assimilation of the microwave sounder MWHS-2 onboard FY-3C in the ECMWF numerical weather prediction system. *IEEE Trans. Geosci. Remote Sens.*, 56(6):3333–3349, 2018.

G. W. Petty. *A first course in atmospheric radiation*. Sundog Publishing, Madison, Wisconsin, 2nd edition, 2006.

C. Prigent, J.-P. Wigneron, W. B. Rossow, and J. R. Pardo-Carrion. Frequency and angular variations of land surface microwave emissivities: Can we estimate ssm/t and AMSU emissivities from SSM/I emissivities? *IEEE: TRANSACTIONS ON GEOSCIENCE AND REMOTE SENSING*, 38(5):2373–2386, 2000.

R. Saunders, J. Hocking, E. Turner, P. Rayer, D. Rundle, P. Brunel, J. Vidot, P. Roquet, M. Matricardi, A. Geer, N. Bormann, and C. Lupu. An update on the rttov fast radiative transfer model (currently at version 12). *Geoscientific Model Development*, 11(7):2717–2737, 2018. doi: 10.5194/gmd-11-2717-2018. URL https://www.geosci-model-dev.net/11/2717/2018/.

P. Weston, N. Bormann, A. Geer, and H. Lawrence. Harmonisation of the usage of microwave sounder data over land, coasts, sea ice and snow: First year report. EUMETSAT/ECMWF Fellowship Programme Research Report 45, ECMWF, 2017.

P. Weston, A. Geer, and N. Bormann. Investigations into the assimilation of AMSU-A in the presence of cloud and precipitation. EUMETSAT/ECMWF Fellowship Programme Research Report 50, ECMWF, 2019.